X-ray irradiated LDPE/PP blends with high mechanical and dielectric performance

Ümit Alkan,[1] Mehmet Kılıç [ID],[2] Yaşar Karabul,[2] Mustafa Çağlar,[3] Orhan İçelli,[2] Zeynep Güven Özdemir[2]

[1]Department of Computer Engineering, Istanbul Gelişim University, Istanbul 34215, Turkey
[2]Department of Physics, Yildiz Technical University, Istanbul 34220, Turkey
[3]Department of Medical Physics, Institute of Health Sciences, Istanbul Medipol University, İstanbul 34810, Turkey
Correspondence to: M. Kılıç (E-mail: kilic-m@hotmail.com)

ABSTRACT: In this study, the influences of polypropylene (PP) additive (varying from 20% to 80% wt) and low dose X-ray irradiation (changing from 25 to 100 Gy) on the mechanical and dielectric properties of low-density polyethylene (LDPE) were investigated. LDPE/PP film blends were prepared by hot press technique. While the highest Young modulus and tensile strength were observed for the 20%LDPE/80%PP blend at 25 Gy X-ray irradiation, the same blend had the highest energy at break and percentage strain at break values for 50 Gy X-ray exposure. These results also indicated a chain scission in the material. The differential scanning calorimetry curves also indicated a chain scission and crosslinking effects in the blends due to X-ray irradiation. Hence, the higher concentration of PP additive and exposure of low dose X-ray resulted in a polymer composite with high mechanical performance. On the other hand, the dielectric investigations revealed that the 25 Gy X-ray irradiated 20%LDPE/80%PP blend may also attract attention for capacitor applications due to its increased static dielectric constant and reduced dielectric loss. © 2018 Wiley Periodicals, Inc. J. Appl. Polym. Sci. **2018**, *135*, 46571.

INTRODUCTION

In recent years, studies on the low cost, flexible, and good processed polymer composites with high dielectric constant have been paying much attention for both industrial applications and academic research.[1,2] High-performance polymers, which possess a low dielectric loss, high dielectric constant, and flexibility, have attracted great interest due to their potential applications in numerous cutting-edge industries, including microelectronics, aviation, and aerospace.[3,4] Low-density polyethylene (LDPE) composites are widely used in industry due to their lightweight and excellent electrical, mechanical, and thermal properties. The mechanical and dielectric properties of LDPE polymer can be improved by reinforcing the polymer matrix with fillers, such as polymers, fibers, or platelets.[5,6] For example, Khanam et al. investigated the effect of Al_2O_3 addition to the flexible recycled LDPE. While the mechanical properties of the recycled LDPE got worse due to the Al_2O_3 dopant, the relative permittivity and dielectric loss increased. They explained the decrease in the mechanical properties of LDPE/Al_2O_3 composites with the occurrence of poor surface contact with the polymer and agglomeration.[7] Gaska et al. also researched the

mechanical and electrical properties of LDPE/graphene nano platelets (GnP) composites. They showed that as the plane conductivity decreases for the low concentrations of GnP, the mechanical parameters such as Young's modulus and tensile strength decrease with GnP doping.[8] On the other hand, Sharma et al. reported that the dielectric constant of pure LDPE decreases with cenosphere filling.[9] Among the wide variety of fillers and dopants, polypropylene (PP) has a special place in the industrial sense. As is known, PP has been used as an industrial polymer due to its feasible processing and chemical resistance. The mechanical blending of LDPE and PP, if they result in a combination of the mechanical performance of both components, may be a more economical and easier method for generating new polymeric materials for particular applications.[10,11] The mechanical properties of LDPE/PP blends have been studied by Shan et al. and Salih et al. The mechanical properties of the blends of LDPE with the homogenous PP and block copolymer PP have been investigated by Shan et al. They reported that the tensile strength and elastic modulus of the blends monotonically increase with increasing PP concentrations.[12] Salih et al. also studied the mechanical properties of LDPE/PP and HDPE/PP polymer blends. They showed that the mechanical properties

of LDPE and HDPE, except for elongation parameter, increase with increasing PP dopant.[13] In this context, the LDPE/PP polymer blends have been investigated mostly in the context of their mechanical properties but their dielectric properties have not been investigated in details till now.

The interaction between polymers and ionizing electromagnetic rays such as γ-rays and X-rays also enabled us to obtain a polymer and polymer composites with desirable mechanical and dielectric properties. It is well-known that the interaction of polymeric materials with ionizing radiation significantly changes their physical, chemical, and structural properties and therefore leading to the formation of reactive intermediates including excited states, ions, and free radicals. In addition, knowing the behavior of polymers after receiving high-energy irradiation is of importance for an extensive approach to the lifetime prediction of polymer materials in use.[14] For example, γ radiations can result in significant modifications in the properties of polymers being treated. These treatments have been known and utilized broadly in the study of bio-applications, semiconductor detectors, and polymer-based devices.[15,16] The effects of ionizing radiation on the molecular relaxation of polyethylene have been the subject of recent publications. Suarez *et al.* reported that γ irradiation causes a crosslinking and chain scission in the polyolefins/LDPE samples for the low and high doses of gamma rays, respectively. The mechanical performance of the samples such as hardness improved with increasing gamma doses.[17] Sabet *et al.* also studied the effect of electron beam irradiation on the mechanical properties of LDPE. They observed an important improvement on the tensile strength with increasing electron beam doses. On the other hand, they did not find a significant change in the dielectric constant and dielectric loss due to electron beam irradiation.[18] Maysa investigated the influence of gamma rays varying up to 250 kGy dose on the mechanical properties of LDPE/bromobutyl composites. He showed that the gamma rays-irradiated samples with rays have better mechanical performance relative to pristine ones.[19] Hence, it has been revealed that there is no study in the scientific literature that examined both the dielectric and mechanical properties of the blend of LDPE/PP samples in the context of application of low dose X-rays. From this point of view, this work has been devoted to develop the mechanical and dielectric properties of LDPE by both doping different rates of PP and X-ray irradiation. The mechanical and dielectric properties of the blends have been analyzed by stress–strain tests and impedance spectroscopy measurements, respectively.

EXPERIMENTAL

Materials
LDPE [Product #: I22-19T; melting point of 105 °C, density of 0.919 g/cm^3, and melt flow index of 22 g/10 min (190 °C/2.16 kg)] and PP [Product #: MH418; melting point of 163 °C, density of 0.905 g/cm^3, and melt flow index of 4.7 g/10 min (230 °C/2.16 kg)] have been obtained from Petkim Industry (Turkey).

Preparation of LDPE/PP Thick Films
In this work, LDPE and PP powders have been mixed with different PP (20%, 40%, 60%, and 80%) concentrations. LDPE and LDPE/PP composites have been prepared by a hot press

process. Hot press procedure involved a pre-heating step for 20 min at 413 K and 433 K for pure LDPE and LDPE/PP composites, respectively, followed by compression for 10 min at the same temperatures under 15 MPa pressure. Finally, homogeneous films have been obtained for each melting mixture. At the end of the hot press process, thick films have been cooled in the flow of cold water. While the thicknesses of the samples, measured by using a Mitutoyo micrometer, were varying between 72 and 105 μm, the diameter of the samples was 24 mm.

X-ray Irradiation Procedure of the Thick Films
The radiation has been generated for each film on a Linac (Varian TrueBeam STX 2.0) using nominal energies as 6 MV X-rays. A fixed-beam geometry has been used at 0° angle, employing one beam blocked field. The irradiation has been made at SAD (Source Axis Distance) of 100 cm and 40 × 40 cm^2 field size using solid water phantom. Films have been placed in 1.5 cm depth at solid water phantoms. At first, the films have been irradiated 2500 MU for 25 Gy since linac has been calibrated 1 cGy/MU at maximum dose depth. Then, 5000 MU and 10,000 MU have been used for 50 and 100 Gy, respectively. A 600 MU/min has been chosen as a static dose rate for each irradiation.

Structural Characterization of the Thick Films
Fourier-transform infrared (FTIR) spectrum of each composite has been obtained by a Spectrum 100 FTIR spectrometer (Perkin Elmer Inc., Waltham, MA) operated in transmission mode with the spectral region from 4000 to 600 cm^{-1}.

Characterization of Mechanical Properties of the Thick Films
The mechanical response of the thick films has been evaluated by using "Lloyd Instruments LF Plus Single Column Universal Materials Testing Machine" with a crosshead speed of 50 mm/min at 23 ± 3 °C.

Characterization of Dielectric Properties of the Thick Films
The dielectric spectrum of the samples has been determined by HP 4194A Impedance Analyzer between 100 Hz and 15 MHz frequency with a high accuracy of 0.17% at room temperature. The samples have been placed between two gold electrodes. The diameters of the electrodes were 20 mm. The experimental results have been transferred to a computer with GPIB data cable and simultaneously recorded by the computer.

RESULTS AND DISCUSSION

FTIR Spectrum Analysis of the Thick Films
Figure 1 shows the FTIR spectra of the LDPE, PP, and LDPE/PP samples which have been cut out from the films. The transmittances of irradiated LDPE and PP have been compared with the transmittance of non-irradiated material.

For the pure LDPE [Figure 1(a)], the characteristic double strong peaks at 2914 and 2848 cm^{-1} correspond to asymmetric stretching vibration of C—H groups and the symmetric stretching vibration of C—H. The peak at 1463 cm^{-1} indicated the C—H bending deformation vibration in CH$_2$ groups. The medium peak at 1377 cm^{-1} also indicated the CH$_3$ symmetric deformation. The sharp peak observed at 718 cm^{-1} corresponds to the characteristic C—C rocking vibration of long chains of CH$_2$ groups.[20,21]
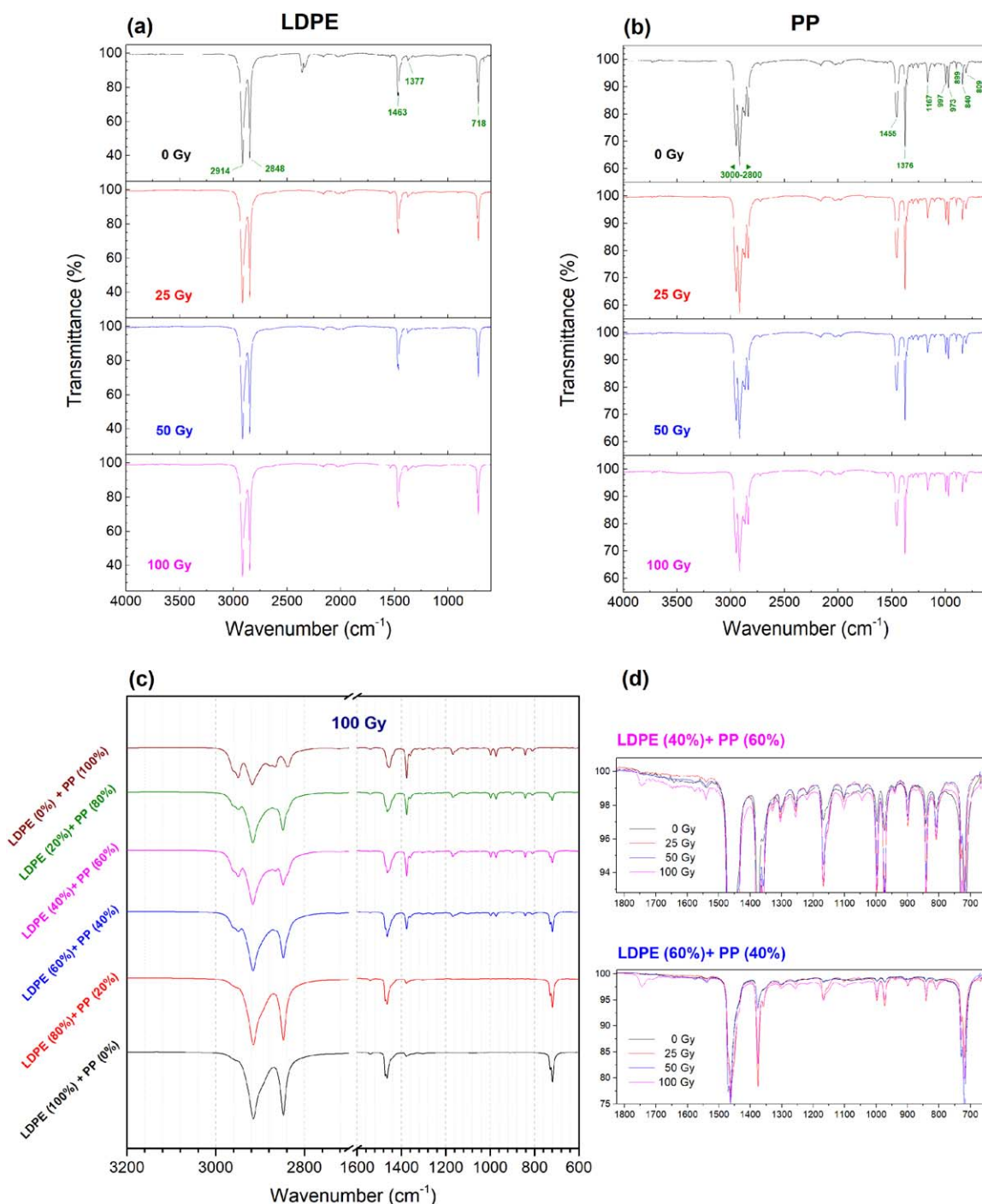
Figure 1. FTIR spectra of (a) pure LDPE, at different X-ray irradiation doses, (b) pure PP, at different X-ray irradiation doses, (c) LDPE/PP blends for 100 Gy X-ray irradiation, and (d) 40% and 60% PP additive LDPE/PP blends at different X-ray irradiation doses. [Color figure can be viewed at wileyonlinelibrary.com]

The characteristic strong peaks between 3000 and 2800 cm^{-1} indicate the asymmetric C—H stretching vibrations and the symmetric C—H stretching vibrations in CH_3, CH_2, and CH groups for the pure PP [see Figure 1(b)].[22] The strong peak at 1455 and 1376 cm^{-1} also indicated the asymmetric and the symmetric scissoring vibrations of the methyl group (CH_3), respectively.[23] The peak observed at 1167 cm^{-1} corresponds

to the C—C chain stretching, C—H wagging, and CH_3 rocking vibrations. The sharp peaks at 997, 973, and 899 cm^{-1} showed the CH_3 rocking and the C—C chain stretching vibrations. The peak at 840 cm^{-1} also showed the CH_2 rocking and the C—CH_3 stretching vibrations. The medium peak observed at 809 cm^{-1} indicated the C—C stretching and CH_2 rocking.[24–26]
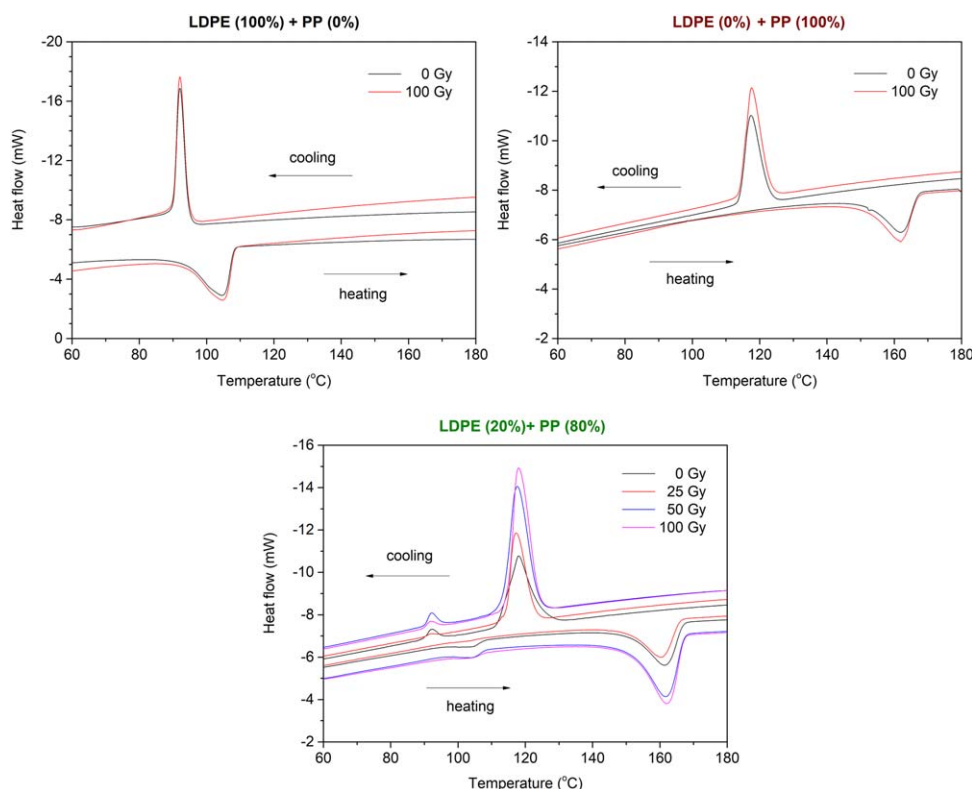
Figure 2. The DSC heating and cooling curves for (a) LDPE(100%)+PP(0%), (b) LDPE(0%)+PP(100%), and (c) LDPE(20%)+PP(80%) samples between 0 and 100 Gy irradiation conditions. [Color figure can be viewed at wileyonlinelibrary.com]

No significant differences have been observed between the FTIR spectra of non-irradiated (i.e., pristine) blends while some minor differences in the intensity and transmittance have been recorded after irradiation. When the influence of PP additive on FTIR spectrum of LDPE is examined, it has been observed that the characteristics LDPE peaks are predominant for the LDPE/PP blends with low PP additives. As expected, the characteristic FTIR peaks of PP became more prominent for LDPE/PP blends with higher PP additives [Figure 1(c)]. Depending on the concentration of the additive made, small deviations occurred in the characteristic peaks of LDPE and PP [Figure 1(d)]. Similar to pure LDPE and PP, the X-ray radiation did not cause a significant change in the FTIR spectrum of the blends. Some small differences in the percentages of intensity and transmittance occurred due to X-ray irradiation. The minor change in the intensity and transmittance of these peaks implied the occurrence of chain scission and crosslinking.[27]

Differential Scanning Calorimetry Analysis of the Thick Films

Differential scanning calorimetry (DSC) curves of the samples were obtained by Perkin-Elmer DSC 8500. Samples with masses of approximately 1.7–2.1 mg were heated from 20 to 200 °C at a rate of 10 °C/min in order to eliminate the thermal history, cooled to 20 °C at the rate of 10 °C/min, and then re-heated and re-cooled under the same conditions mentioned earlier. Three different samples were analyzed for each sample. The melting and crystallization data were determined from the second scan.

The DSC heating and cooling curves obtained from the second scan are shown in Figure 2. The influence of X-ray irradiation on the heating and cooling curves for pure LDPE and pure PP are shown in Figure 2(a,b), respectively. Additionally, the impact of X-ray irradiation doses on the heating and cooling curves of the composite which includes 80% PP additive is given in Figure 2(c).

As shown in Figure 2(a,b), pure LDPE and PP exhibit two single peaks observed at the heating and cooling process which correspond to the melting and crystallization behaviors of the samples. On the other hand, the LDPE(20%)+PP(80%) blend displayed two double peaks that represent their composite nature [see Figure 2(c)]. The small low-temperature melting and crystallization peaks observed for the composite verified the presence of the low concentration of LDPE in the composite.

Some characteristic temperatures including melting and crystallization temperatures, T_m and T_c, and the melting enthalpy (i.e., heat of fusion), ΔH_m were derived from DSC curves and listed in Table I. As is known, melting temperature depends on the crystalline properties of the polymer and the melting enthalpy is defined as the amount of the crystalline phase with respect to the total mass of the polymer (crystallinity degree). In Table I, while T_i is the initial temperature of the melting peak, T_f is final melting temperature. ΔT is known as the melting temperature range and defined as the difference between T_f and T_i. The melting temperature, T_m, was taken as the maximum of the endothermic peak. The melting enthalpy, ΔH_m was also calculated from specific heat capacity, ΔC_P. The crystallization

Table I. Characteristic Temperatures, Specific Heat Capacity and Melting Enthalpy for the Samples Derived from DSC Spectra

Sample	T_i (°C)	T_f (°C)	T_m (°C)	ΔT (°C)	ΔC_p (j/g °C)	ΔH_m (j/g)	T_c (°C)
LDPE(100%)+PP(0%) 0 Gy	86.94	115.10	104.63	28.16	4.389	123.59	92.08
LDPE(100%)+PP(0%) 100 Gy	86.83	112.71	104.75	25.88	4.405	114.00	92.07
LDPE(0%)+PP(100%) 0 Gy	140.77	171.75	162.03	30.98	1.415	43.84	117.43
LDPE(0%)+PP(100%) 100 Gy	139.32	171.75	161.83	32.43	2.050	66.48	117.63
LDPE(20%)+PP(80%) 0 Gy	143.49	171.39	161.45	27.90	2.824	78.79	118.01
LDPE(20%)+PP(80%) 25 Gy	142.58	171.93	160.60	29.35	1.387	40.71	117.27
LDPE(20%)+PP(80%) 50 Gy	135.05	171.15	161.78	36.10	2.364	85.34	117.65
LDPE(20%)+PP(80%) 100 Gy	137.15	177.00	162.12	39.85	2.624	104.57	118.07

The melting points of the blend were determined from the main melting peak.

temperature T_c was determined from the maximum value of the exothermic peak.

As shown in Table I, the pristine LDPE and PP have the melting temperatures of 104.63 and 162.03 °C which are consistent with their catalog melting information given in "Materials" Section. A slight increase in the melting point of pure LDPE was observed due to X-ray irradiation. However, the crystalline temperature of T_c almost did not affect due to irradiation process. This behavior can be associated with the small amount of enhancement of the crystalline properties of the LDPE due to X-ray irradiation. On the other hand, the temperature of the pure PP decreased due to 100 Gy X-ray irradiation. The slight decrease in T_m point suggests a minor degradation caused by chain scission.[28] Since molecular modifications induced by ionizing radiation occur mostly in the amorphous regions and ionizing radiation at low doses does not make a considerable change in the crystalline properties of the polymer, pure LDPE and pure PP showed a minor degradation due to low dose X-ray irradiation. A remarkable modification in the amorphous region can be observed with the introduction of irregularities in the crystalline nature of the polymer due to the occurrence of crosslinking and degradation. According to Spadora et al., such modifications (i.e., degradations) manifest itself as a decrease in both T_m and ΔH_m values in the DSC curves.[29,30] According to Table I, LPDE(20%)+PP(80%) composite achieved a decrease in both T_m and ΔH_m values at 25 Gy X-ray irradiation. For the higher X-ray irradiation doses, the blend displayed higher T_m and ΔH_m values. Hence, this behavior of the LDPE/PP blend for the 25 Gy irradiation dose may the associated with the result of crosslinking and chain scission.[31] From this point of view, it was suggested that 25 Gy X-ray irradiation process may have a critical positive role on the improvement of mechanical performance of LDPE(20%)+PP(80%) blend.

Mechanical Analysis of the Thick Films

The effects of dopant and low dose X-ray irradiation on the mechanical properties of the LDPE have been investigated by using stress–strain curves. As is known, stress is defined as the force per unit area of the sample and strain is the measure of the change in the sample length.

While the effect of the PP additive on the pure LDPE's mechanical response has been shown in $\sigma = f(\varepsilon)$ curves given in Figure 3(a), the influence of X-ray exposure on the mechanical properties of some of the LDPE/PP blends have been depicted in Figure 3(b–f). Additionally, the tensile strain and stress data at break are given along with the related standard deviation values in Figure 3.

Figure 3 shows the typical stress–strain curves of semicrystalline thermoplastics. These curves have four characteristic behaviors: elastic, initial necking, cold drawing (plastic) regions, and fracture point.[32] As shown in Figure 3(a), adding a higher concentration of PP to LDPE increased both the tensile strength, which is a measure of a material to withstand a tensile force and toughness property, which is the ability to absorb energy and undergo extensive plastic deformation without rupturing. On the other hand, X-ray irradiation did not cause an improvement of the mechanical response of pure LDPE expect for 25 Gy. As shown in Table I, the DSC results of LDPE revealed that 100 Gy X-ray irradiation causes only a slight increase in the melting point of LDPE which does not make any considerable change in the crystalline property of the LDPE. Hence, any remarkable change in the tensile properties of LDPE was obtained due to X-ray irradiation. As is seen from Figure 3(b), 25 Gy X-ray irradiation only increased the fracture stress with respect to pristine LDPE. On the other hand, 25 Gy X-ray irradiation enhanced the mechanical performance at the break of the LDPE/PP composites [see Figure 3(d–f)].

Young's modulus, tensile strength, percentage strain at break, and energy at the break parameters have been determined by using $\sigma = f(\varepsilon)$ curves of all samples. The changes in the Young modulus, tensile strength, percentage strain at break, and energy at break values due to PP addition and X-ray exposure have been summarized in three-dimensional graphics given in Figure 4(a–d), respectively.

As shown in Figure 4(a), the highest Young modulus of 102.21 MPa due to PP additive has been achieved for the 40% PP doped LDPE composite. On the other hand, the maximum Young modulus of 172.93 MPa due to X-ray exposure has been obtained for the 25 Gy X-ray irradiated 80% PP added LDPE composite. While the 80% PP additive concentration resulted in the raise of the tensile strength to 34.75 MPa, 25 Gy X-ray irradiation to the same blend (20% LDPE/80% PP) increased the tensile strength to its maximum value of 37.60 MPa [see Figure
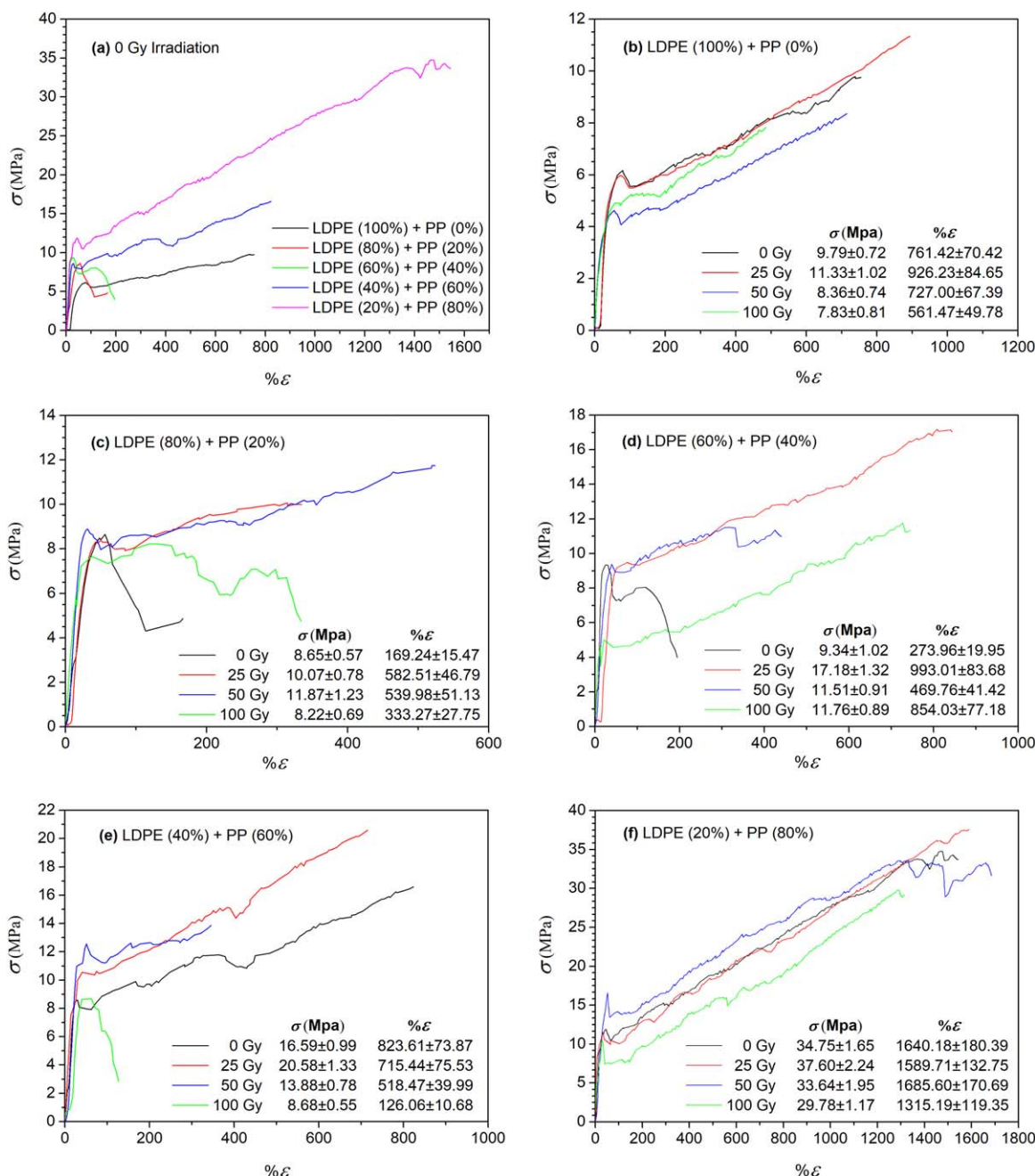
Figure 3. (a) The load–extension curves of the samples at 0 Gy. The $\sigma = f(\varepsilon)$ curves under 0, 25, 50, and 100 Gy X-ray exposure for (b) LDPE(100%)+PP(0%), (c) LDPE(80%)+PP(20%), (d) LDPE(60%)+PP(40%), (e) LDPE(40%)+PP(60%), and (f) LDPE(20%)+PP(80%) samples. [Color figure can be viewed at wileyonlinelibrary.com]

4(b)]. Moreover, 25 Gy X-ray irradiation increased the tensile strength of all pristine samples. The tensile strength performance of the 25 Gy X-ray irradiated sample is also in good agreement with the DSC results of the blend given in Table I. Since observation of the decrease in T_m and ΔH_m values of the LDPE(20%)+PP(80%) blend makes the blend high mechanical performance material. Since X-ray irradiation process increased the tensile strength values for all samples, it was deduced that X-ray irradiation may cause a degradation of the polymers which results in a chain scission. Because, as the chain scission occurs, the average molecular chain length of the blends

decreases that enables a production of crystallites in the blends which yield an increase in the degree of crystallinity of the samples. Among all pristine samples, the highest percentage strain at break has been observed for the 20% LDPE/80% PP composite. Furthermore, it has been revealed that the percentage strain at break value increased to its highest value for the 50 Gy X-ray irradiated 20% LDPE/80% PP composite [see also Figure 4(c)]. Furthermore, as shown in Figure 4(d), the X-ray irradiation process resulted in the highest energy at break values for the pure PP under the influence of 25 Gy irradiation. On the other hand, among all irradiated samples, the highest energy at break
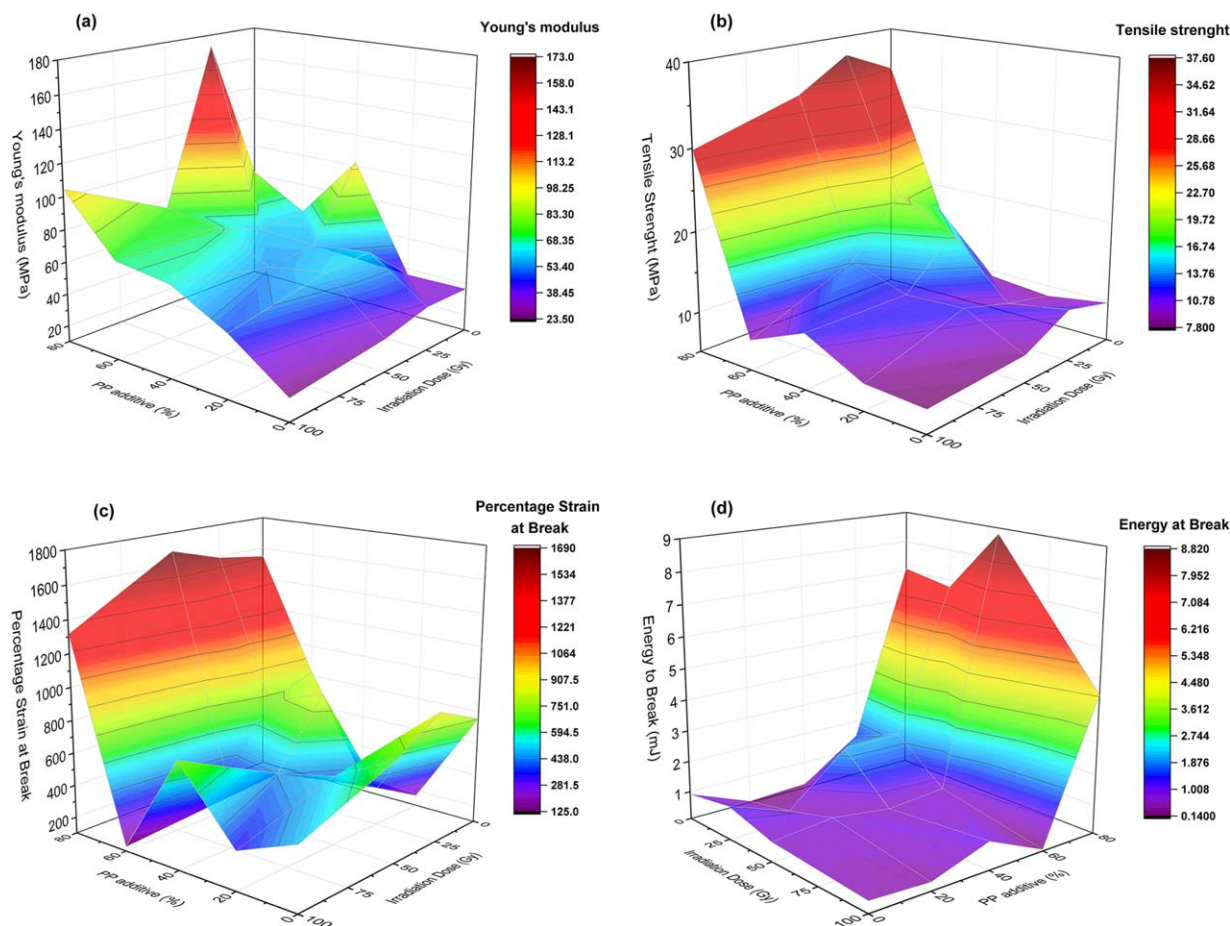
Figure 4. The influence of PP additive and X-ray irradiation on (a) The Young's modulus, (b) tensile strength, and (c) percentage strain at break, and (d) energy at the break for all samples. [Color figure can be viewed at wileyonlinelibrary.com]

value has been recorded for the 80% PP doped LDPE composite at 50 Gy X-ray irradiation dose. In this context, it has been revealed that the specimens exposed to X-rays have become less fragile than pristine ones.

Dielectric Analysis of the Thick Films

The frequency dependence of the dielectric properties of the materials is often presented in terms of complex dielectric constants. The frequency dependent complex dielectric constant $\varepsilon^*(f)$ is defined by

$$\varepsilon^*(f) = \varepsilon'(f) + i\varepsilon''(f) \tag{1}$$

where $\varepsilon'(f)$ and $\varepsilon''(f)$ represent the real and imaginary components of the complex dielectric function, respectively. The real and imaginary components of the complex dielectric function have been calculated by the following relations

$$\varepsilon' = \frac{Cd}{A\varepsilon_0} \tag{2}$$

$$\varepsilon'' = \frac{Gd}{A\varepsilon_0} \tag{3}$$

$$\varepsilon'' = \varepsilon' \tan\delta \tag{4}$$

where C is the capacitance, G is the conductance, and $\tan\delta$ is the loss tangent. The parameters A and d are the active surface area of the electrodes and the thickness of the samples, respectively. The frequency dependences of the real and imaginary parts of the complex dielectric function for the samples with different PP contents for zero Gy X-ray exposure have been shown in Figure 5.

As shown in Figure 5, PP doping decreased the magnitude of the real component of the complex dielectric function. The lowest ε' has been obtained for the 40% PP doped LDPE blend. According to Figure 5(a), the real parts of the complex dielectric function of pure LDPE and its blends were independent of frequency between 100 Hz and a few MHz. We called this frequency independent ε' as static dielectric constant. The upper limit of the frequency independent behavior of ε' was extended by PP doping from 1.33 to 2.24 MHz except for 80% PP added blend. On the other hand, the imaginary component of the complex dielectric function considerably decreased with the 40% and 60% PP doping concentration at high frequencies [see Figure 5(b)]. In addition, it has been observed that the relaxation peak shifted toward the higher frequencies relative to pure LDPE for the additive concentrations of 40% and higher. Moreover, since the relaxation frequencies, at which the maximum dielectric loss has been detected, was between 3 and 10 MHz, the relaxation process can be considered as orientational/dipolar relaxation.
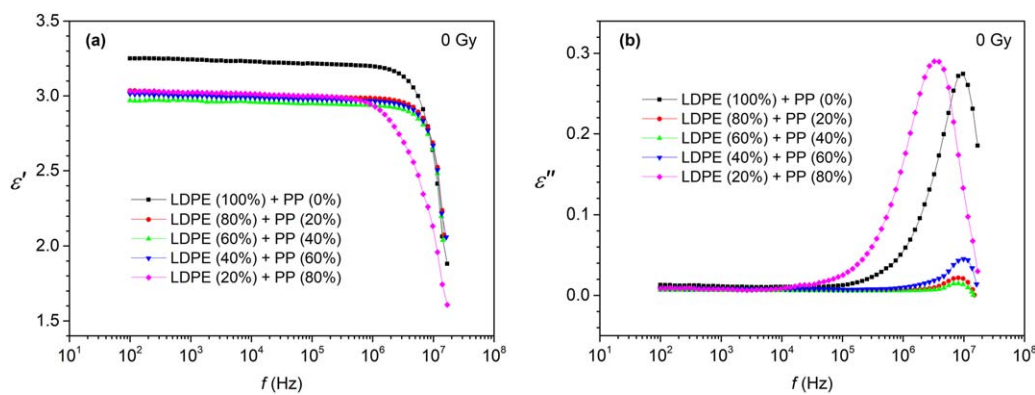
Figure 5. The frequency dependences of the (a) real and (b) imaginary components of the ε* of each sample for 0 Gy. [Color figure can be viewed at wileyonlinelibrary.com]
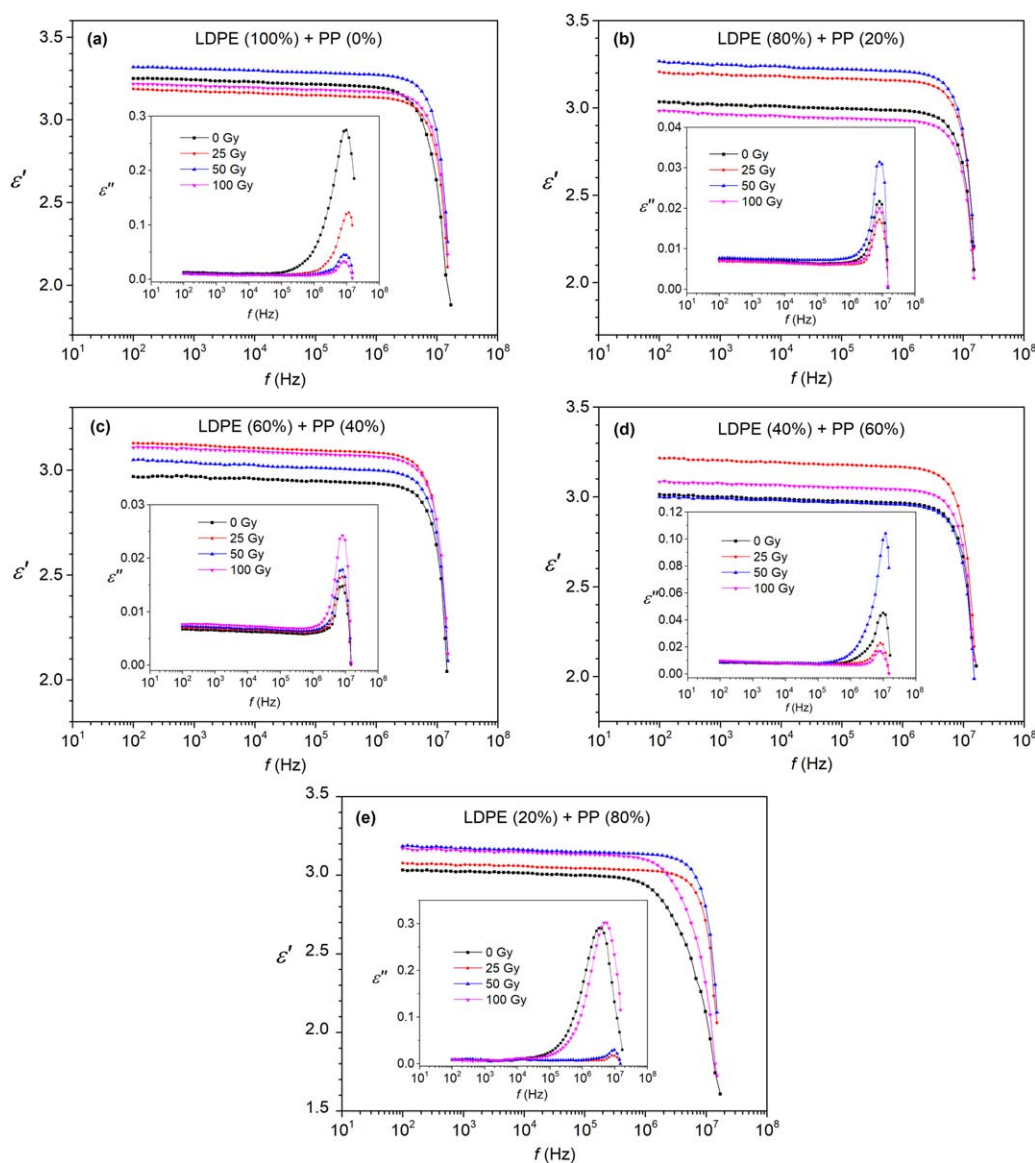

Figure 6. The influence of X-ray irradiation on the ε′ versus frequency and ε″ versus frequency curves for (a) LDPE(100%)+PP(0%), (b) LDPE(80%)+PP(20%), (c) LDPE(60%)+PP(40%), (d) LDPE(40%)+PP(60%), and (e) LDPE(20%)+PP(80%). [Color figure can be viewed at wileyonlinelibrary.com]

The influences of X-ray application on the dielectric properties of the samples have also been investigated. The frequency dependences of the dielectric parameters for the samples under the influence of various X-ray doses have been shown in Figure 6(a–d).

As is seen from Figure 6(a), application of low dose X-ray radiation to pure LDPE in the order of 25 and 100 Gy decreased both the ε' and ε'' parameters for the low and high frequencies, respectively. On the other hand, the increase in ε' with increasing X-ray dose for the blends can be explained by the occurrence of the ionization or excitation of the electrons in atoms or the displacements of atoms for their original equilibrium site to neighboring lattice sites. The last situation also provides the existence of freely moving or partially bonded charge carriers to some trapping centers in the composite material medium. Hence, application of low dose X-ray to the LDPE/PP composites may cause a crosslinking or chain scission in the material. On the other hand, the increase in the magnitude of the dielectric loss peak with X-ray irradiation indicated a crosslink deformation in the blends.[33] Moreover, the samples including pure PP exhibited a sharp and high-intensity dielectric loss peak which points out a molecular vibration. Especially, it has been observed that the dielectric loss peak becomes very sharp and high for 40% PP doped LDPE blend as the X-ray irradiation dose increases.

CONCLUSIONS

In the present work, the LDPE/PP blend polymer thick films have been prepared with different weight ratios of PP varying from 20% to 80% by hot press technique. Then, the samples have been exposed to the low dose X-rays varying between 25 and 100 Gy. The microstructure of the samples including the pristine and irradiated ones has been analyzed by FTIR measurements. Tensile properties such as Young's modulus, tensile strength, percentage strain at break, and energy at break values have been measured by using $\sigma = f(\varepsilon)$ curves. The dielectric properties such as static dielectric constant and dielectric loss have been determined within 100 Hz to 15 MHz frequency interval by complex impedance measurements. It has been understood that the higher concentration of PP additive (80% wt) and X-ray irradiation dose of 25 Gy play a significant role in the mechanical properties as well as dielectric properties of the LDPE. It has been revealed that the 25 Gy X-ray irradiated 20%LDPE/80%PP composite may be suggested as a promising dielectric material with high dielectric constant, reduced dielectric loss, and high mechanical performance for the capacitor applications.

ACKNOWLEDGMENTS

REFERENCES

1. Alkan, Ü.; Kılıç, M.; Karabul, Y.; Yamak, H. B.; Okutan, M.; İçelli, O. *J. Nanoelectron. Optoelectron.* **2016**, *11*, 343.

2. Moharana, S.; Mishra, M. K.; Behera, B.; Mahaling, R. *Polym. Sci., Ser. A* **2017**, *59*, 405.

3. Chi, Q.; Ma, T.; Dong, J.; Cui, Y.; Zhang, Y.; Zhang, C.; Xu, S.; Wang, X.; Lei, Q. *Sci. Rep.* **2017**, *7*, 1.

4. Zheng, M.-S.; Zha, J.-W.; Yang, Y.; Han, P.; Hu, C.-H.; Dang, Z.-M. *Appl. Phys. Lett.* **2016**, *109*, 072902.

5. Ayandele, E.; Sarkar, B.; Alexandridis, P. *Nanomaterials* **2012**, *2*, 445.

6. Ghafarizadeh, S.; Fréchette, M.; David, E. *Polym. Plast. Technol. Eng.* **2018**, *57*, 327.

7. Khanam, P. N.; Al-Maadeed, M.; Mrlik, M. *J. Mater. Sci. Mater. Electron.* **2016**, *27*, 8848.

8. Gaska, K.; Xu, X.; Gubanski, S.; Kádár, R. *Polymers* **2017**, *9*, 11.

9. Sharma, J.; Chand, N.; Bapat, M. *Results Phys.* **2012**, *2*, 26.

10. Shanks, R. A.; Li, J.; Yu, L. Imaging and Image Analysis Applications for Plastics: A Volume in Plastics Design Library; Elsevier Publishing: Amsterdam, the Netherlands, **1999**; p 59.

11. Su, B.; Zhou, Y.-G.; Wu, H.-H. *Nanomater. Nanotechnol.* **2017**, *7*, 1.

12. Shan, G.-F.; Yang, W.; Xie, B.-H.; Yang, M.-B. *J. Macromol. Sci. Part B: Phys.* **2007**, *46*, 963.

13. Salih, S. E.; Hamood, A. F.; Alsabih, A. H. *Mod. Appl. Sci.* **2013**, *7*, 33.

14. Zegaoui, A.; Wang, A.-R.; Dayo, A. Q.; Tian, B.; Liu, W.-B.; Wang, J.; Liu, Y.-G. *Radiat. Phys. Chem.* **2017**, *141*, 110.

15. Daoudi, M.; Raouafi, A.; Chtourou, R.; Hosni, F. *J. Alloys Compd.* **2017**, *728*, 1165.

16. Lim, J.; Lee, Y.; Yang, S. A.; Choi, G. P.; Bu, S. D. *J. Lumin.* **2017**, *188*, 188.

17. Suarez, J. C. M.; da Costa Monteiro, E. E.; Mano, E. B. *Polym. Degrad. Stab.* **2002**, *75*, 143.

18. Sabet, M.; Hassan, A.; Ratnam, C. T. *Polym. Bull.* **2012**, *68*, 2323.

19. Maysa, A. *J. Thermoplast. Compos. Mater.* **2014**, *27*, 364.

20. Alkan, U.; Özcanlı, Y.; Alekberov, V. *Fibers Polym.* **2013**, *14*, 115.

21. Santhoskumar, A.; Komaragounder, P.; Sharma, S. K.; Nayak, S. K. *J. Bioremediat. Biodegrad.* **2010**, *1*, 12010.

22. Mathakari, N.; Bhoraskar, V.; Dhole, S. *Radiat. Effects Defects Solids* **2014**, *169*, 779.

23. Abdel-Hamid, H. *Solid State Electron.* **2005**, *49*, 1163.

24. Alkan, Ü.; Karabul, Y.; Bulgurcuoğlu, A. E.; Kılıç, M.; Özdemir, Z. G.; İçelli, O. *e-Polymers* **2017**, *17*, 417.

25. Sinha, D.; Swu, T.; Tripathy, S.; Mishra, R.; Dwivedi, K.; Fink, D. *Radiat. Effects Defects Solids* **2003**, *158*, 531.

26. Türkçü, H. N. Master of Science Thesis, The Institute of Engineering And Sciences of Bilkent University, Ankara, **2004**.

Applied Polymer
JOURNAL OF   SCIENCE

27. Raghu, S.; Archana, K.; Sharanappa, C.; Ganesh, S.; Devendrappa, H. *J. Radiat. Res. Appl. Sci.* **2016**, *9*, 117.

28. Oliani, W. L.; Parra, D. F.; Fermino, D. M.; Riella, H. G.; Lima, L. F. C. P.; Lugao, A. B. In 2009 International Nuclear Atlantic Conference-INAC, Rio de Janeiro, RJ, Brazil, **2009**, 1–11.

29. Spadaro, G. *Eur. Polym. J.* **1993**, *29*, 851.

30. Spadaro, G.; Valenza, A. *J. Therm. Anal. Calorim.* **2000**, *61*, 589.

31. Reinholds, I.; Kaļķis, V.; Zicāns, J.; Merijs-Meri, R.; Pavlovica, I. *Mater. Sci. Appl. Chem.* **2012**, *25*, 16.

32. Xu, M.-M.; Huang, G.-Y.; Feng, S.-S.; McShane, G. J.; Stronge, W. J. *Polymers* **2016**, *8*, 77.

33. Al Lafi, A. G. *Polym. Bull.* **2012**, *68*, 2269.

ADVANCED SCIENCE NEWS
advancedsciencenews.com